The World of Quantum Mechanics
Assignment 2, Computational Physics

Federico Rossi

March 2024

Abstract

This report presents a study of quantum mechanical systems using numerical methods. The Schrödinger equation is solved for the case of a particle in a one dimensional box with various potential configurations. Initially, the focus lies at the time-independent solutions for the free particle where numerical and analytical solutions are compared. The eigenfuctions determined in this way are used as a base to expand the wave function and study the time evolution, together with forward Euler and Crank-Nicolson schemes. A potential barrier is then introduced in the central area of the box and the effect on eigenvalues and eigenfunctions is studied, with particular focus on the eigenvalues lower than the potential barrier. Finally, the case of a double barrier or barrier and well is discussed, looking at effect of the barrier values on the tunneling probabilities. In the last section, the case of an oscillating well is considered, that is able enforce probability transitions by coupling the respective states.

1 Particle in a box

We will start studying the case of a particle of mass m in a confined 1D space $x \in [0, L]$. Since the square module of the wave function represent the probability of finding the particle in that position, outside the confined space we will have $\Psi(x, t) = 0$. Given the continuity of the wave function, we require $\Psi(0, t) = \Psi(L, t) = 0$.
The time-dependent Schrödinger equation reads

$$-\frac{\hbar^2}{2m}\frac{\partial^2\Psi}{\partial x^2} = i\hbar\frac{\partial\Psi}{\partial t} \tag{1}$$

1.1 Change of notation

Before we start, it is convenient to use a new set of variables $x' = x/L$ and $t' = t/t_0$ with $t_0 = 2mL^2/\hbar$. Since $\partial t = t_0\partial t'$, Eq. 1 becomes

$$-\frac{\hbar^2}{2mL^2}\frac{\partial^2\Psi}{\partial x'^2} = i\hbar\frac{\hbar}{2mL^2}\frac{\partial\Psi}{\partial t'} \implies -\frac{\partial^2\Psi}{\partial x'^2} = i\frac{\partial\Psi}{\partial t'} \tag{2}$$

The time-independent Schrödinger equation reads instead

$$-\frac{\hbar^2}{2m}\frac{\partial^2\psi_n}{\partial x^2} = E_n\psi_n \tag{3}$$

and again substituting $x' = x/L$ and $\lambda_n = E_n\, 2mL^2/\hbar^2$ gives

$$-\frac{\partial^2\psi_n}{\partial x'^2} = \lambda_n\psi_n \tag{4}$$

Thanks to these substitutions the space is now $x' \in [0, 1]$ and we are requiring that $\Psi(0, t) = \Psi(1, t) = 0$. We could have chosen any other combination of $x' = \alpha x/L$ with non-zero α and obtain dimensionless equations in $[0, \alpha]$.

1.2 Finite difference scheme

We can rewrite the second derivative of ψ in Eq. 4 using the second-order centered derivative formula

$$-\frac{\psi_{n+1} - 2\psi_n + \psi_{n-1}}{\Delta x'^2} = \lambda_n \psi_n \tag{5}$$

that can be rewritten in matrix form as $\mathbf{H}\boldsymbol{\psi} = \boldsymbol{\lambda}\boldsymbol{\psi}$

$$\frac{1}{(\Delta x')^2}\begin{pmatrix} 2 & -1 & 0 & \dots & 0 \\ -1 & 2 & -1 & \dots & 0 \\ 0 & -1 & 2 & \ddots & \vdots \\ \vdots & \vdots & \ddots & \ddots & -1 \\ 0 & 0 & \dots & -1 & 2 \end{pmatrix}\begin{pmatrix} \psi_1 \\ \vdots \\ \vdots \\ \vdots \\ \psi_{N-1} \end{pmatrix} = \begin{pmatrix} \lambda_1 & 0 & 0 & \dots & 0 \\ 0 & \lambda_2 & 0 & \dots & 0 \\ 0 & 0 & \lambda_3 & \dots & 0 \\ \vdots & \vdots & \vdots & \ddots & \vdots \\ 0 & 0 & 0 & \dots & \lambda_{N-1} \end{pmatrix}\begin{pmatrix} \psi_1 \\ \vdots \\ \vdots \\ \vdots \\ \psi_{N-1} \end{pmatrix} \tag{6}$$

Now, diagonalizing $\mathbf{H}$ will provide λ_n as eigenvalues and the corresponding eigenvectors ψ_n. Unless specified differently, the numerical solutions are obtained by using $N = 100$ and consequently $\Delta x = 0.01$.

1.3 Determining the exact solution

Let's discuss the solution of Eq. 4, starting from the Ansatz

$$\psi = Ae^{ikx'} + Be^{-ikx} \implies \psi'' = -k^2\psi \tag{7}$$

Inserting this in Eq. 4 gives $k^2\psi = \lambda\psi$. Imposing the boundary conditions gives

$$0 = \psi(0) = A + B \implies A = -B \tag{8}$$

$$0 = \psi(1) = Ae^{ik} + Be^{-ik} = A(e^{ik} - e^{-ik}) = 2A\sin(k) \implies k = n\pi \tag{9}$$

where now it's clear where the indexing n comes from, giving the eigenvalues $\lambda_n = (n\pi)^2$ and eigenvectors $\psi_n(x') = A_n \sin(n\pi x')$. Finally, to determine A_n we ensure that the L2-norm for $x \in [0, 1]$ is 1

$$1 = \int_0^1 \psi_n^2(x')\mathrm{d}x' = \frac{A_n^2}{2} \implies A_n = \sqrt{2} \tag{10}$$

Thus, giving the final function as $\psi_n(x') = \sqrt{2}\sin(n\pi x')$.

These can be compared to the numerical eigenfunctions by looking at the L2 norm of the difference between the wavefunctions obtained in the two methods and for the ground state this is $2.6\,10^{-13}$ so it's substantially zero. Changing N does not change this significantly, the numerical error of the integration is just increased.

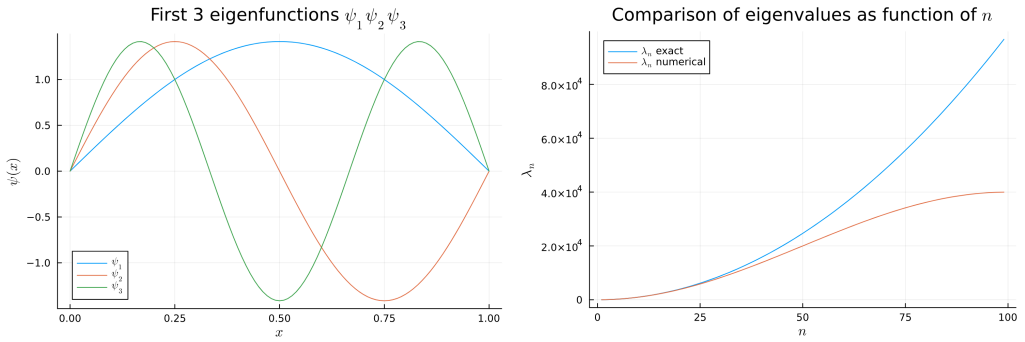

Figure 1: Plot of the first 3 eigenfunctions. After the numerical eigenfunctions are normalized and adjusted in the sign, they overlaps almost perfectly so only one set is represented. The eigenvalues instead are initially overlapped but eventually the numerical ones don't show the parabolic behaviour of the exact ones. Increasing n helps to obtain closer eigenvalues (e.g. the relative error at $n = 50$ decreased from 0.2 to 0.05 when N increased from 100 to 200). All the units are expressed as defined in Sec. 1.1.

1.4 Expansion in eigenfuncitons

Given an initial condition of the wavefunction $\Psi_0 = \Psi(x, t = 0)$, the formal solution of Eq. 1 for a time-independent Hamiltonian is

$$\Psi = \exp\left(-\frac{it}{\hbar}\hat{H}\right)\Psi_0 \tag{11}$$

Suppose that we know the expansion of the initial condition $\Psi_0(x)$ in the eigenfunctions ψ_n as $\Psi_0(x) = \sum_n \alpha_n \psi_n$, then the time evolution can be expressed as

$$\Psi(x,t) = \sum_n \alpha_n \exp\left(-\frac{iE_n t}{\hbar}\right)\psi_n(x) \tag{12}$$

or by using the notation in Sec. 1.1, noticing that $E_n t = \hbar\lambda_n t'$,

$$\Psi(x',t') = \sum_n \alpha_n \exp\left(-i\lambda_n t'\right)\psi_n(x') \tag{13}$$

The coefficients can be obtained projecting the state onto the eigenstates

$$\alpha_n = \langle\psi_n, \Psi_0\rangle = \int \psi_n^*(x')\Psi_0(x')\,\mathrm{d}x' \tag{14}$$

This is also implemented discretizing the integral and using the trapezoidal rule. The same routine can be used to evaluate the projections between the eigenstates, confirming the orthogonality $\langle\psi_n, \psi_m\rangle = \delta_{nm}$.

To test the code we used Eq. 13 to evolve the first exact eigenfunction $\Psi_0(x') = \sqrt{2}\sin(\pi x')$, using Eq. 14, which will give $\alpha_n = \delta_{n1}$. The results shows the expected results, with ψ_1 that is simply changed with a phase, maintaining an L2 norm of 1, since the exponential is unitary. Choosing time $\tau = \pi/\lambda_1$ gives a $\Psi(x', \tau)$ that is again real and simply the opposite of $\Psi_0(x')$, since the phase is $\exp(-i\pi) = -1$.

Now we change the initial condition to a delta function localized in the center $\Psi_0(x') = \delta(x' - 0.5)$, which is implemented as a vector of all zero entries and value $1/\Delta x$ at the

middle point. In this case $\alpha_n = \sqrt{2}\sin(n\pi/2)$ so ± 1 for n odd and 0 for n even. When $t' = 1/\pi$, the exponential becomes $\exp(-i\pi n^2) = -1$, since we only have n odd and n^2 has the same parity, which means that we get back the same delta, with an opposite sign that is not changing the squared module. From the time evolution animation [1], we can see that the evolution is quite complex, with rapid and erratic oscillations but keeps the normalization. The problem is due to the discretization of the problem. In fact, we would really need the whole infinite expansion in the eigenfunctions to describe the delta, which can't be normalized since we have an infinite series of ± 1. From another perspective, we are starting with absolute certainty about the position of the particle, which means that the uncertainty on the velocity and thus the evolution in time is maximum.

2 Box with potential barrier

We will now study the problem with the addition of a potential barrier, constant in time and defined as

$$V(x) = \begin{cases} 0, & \text{for} \quad 0 \leq x < L/3 \\ V_0, & \text{for} \quad L/3 \leq x < 2L/3 \\ 0, & \text{for} \quad 2L/3 \leq x < L \\ \infty, & \text{otherwise} \end{cases} \tag{15}$$

The dimensionless Schrödinger equation now includes the potential $v(x) = t_0 V(x)/\hbar$, with $v_0 = V_0/\hbar$

$$i\frac{\partial \Psi}{\partial t'}(x', t') = \left[-\frac{\partial^2}{\partial x'^2} + v(x')\right]\Psi(x', t') \tag{16}$$

and the time-independent version now reads

$$\left[-\frac{\partial^2}{\partial x'^2} + v(x')\right]\psi_n(x') = \lambda_n \psi_n(x'). \tag{17}$$

The solution of this variant follows the same procedure of Sec. 1.2, with a matrix $\mathbf{H}$ now defined as

$$\mathbf{H} = \frac{1}{(\Delta x')^2}\begin{pmatrix} 2 & -1 & 0 & \dots & 0 \\ -1 & 2 & -1 & \dots & 0 \\ 0 & -1 & 2 & \ddots & \vdots \\ \vdots & \vdots & \ddots & \ddots & -1 \\ 0 & 0 & \dots & -1 & 2 \end{pmatrix} + \begin{pmatrix} v_1 & 0 & 0 & \dots & 0 \\ 0 & v_2 & 0 & \dots & 0 \\ 0 & 0 & v_3 & \dots & 0 \\ \vdots & \vdots & \vdots & \ddots & \vdots \\ 0 & 0 & 0 & \dots & v_{N-1} \end{pmatrix} \tag{18}$$

where $v_k = v(k\Delta x)$.
To check the implementation, the results for $v_0 = 0$ are compared to the results of Sec. 1.2, which are the same. We then move to consider the case of $v_0 = 10^3$. The first 8 eigenvalues are $\lambda_n = 73.076, 73.078, 289.722, 289.748, 638.960, 639.435, 1029.101, 1074.889, \dots$ and in particular we see that the values are increasing but initially we have pairs of very close values and a large difference with respect to the next pair. After $n = 7$ the eigenvalues are more equally spaced, as seen in Fig. 2.

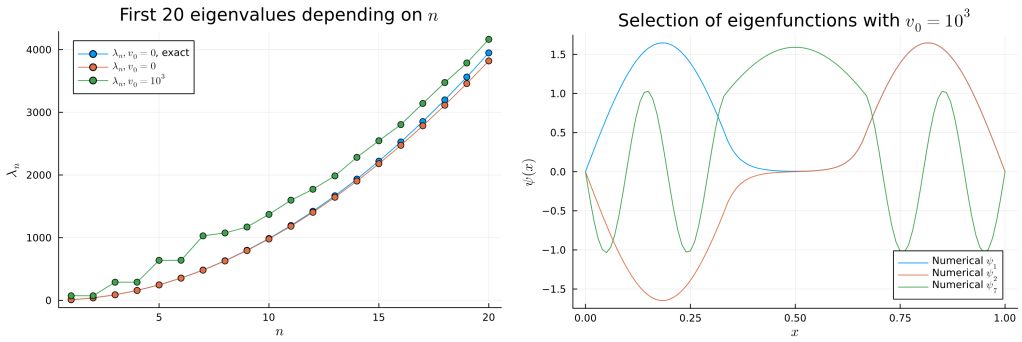

Figure 2: (Left) Plot of the first 20 eigenvalues for the exact and numerical solutions with $v_0 = 0$ and the numerical solutions at $v_0 = 10^3$. The initial almost step-like behaviour can be appreciated for the latter case. (Right) Plot of 3 selected eigenfunctions. ψ_1 and ψ_2 are describing almost the same situation if we look at the squared module. With $n = 7$ we have energy greater than the barrier and we start to include non-zero probability of finding the particle in the barrier.

The motivation is that initially the particle can be found on either side of the barrier and the combinations obtained mixing the two situation are nearly degenerate. When the energy is higher than the energy of the barrier, we can have movement of the particle allowed between the two sides and non-zero probability to find the particle in the barrier, removing the constraint.

We will now evolve the solutions in time, using Eq. 13, starting with a combination of the first 2 eigenfunctions $\Psi_0 = (\psi_1 + \psi_2)/\sqrt{2}$, localized on the right side of the barrier (this can be understood looking at Fig. 2 right). Looking at the animation of the squared module [2], increasing the time gradually increases the probability of finding the particle on the left side at the expenses of the right side, maintaining zero probability on the barrier. In fact, at time $\tau = \pi/(\lambda_2 - \lambda_1)$ the situation is completely inverted, with the squared module entirely concentrated on the left side. In fact,

$$\Psi(t' = 0) = \frac{1}{\sqrt{2}}(\psi_1 + \psi_2) \tag{19}$$

$$\Psi(t' = \tau) = \frac{1}{\sqrt{2}}(e^{-i\pi\frac{\lambda_1}{\lambda_2-\lambda_1}}\psi_1 + e^{-i\pi\frac{\lambda_2}{\lambda_2-\lambda_1}}\psi_2) = \frac{1}{\sqrt{2}}e^{-i\pi\frac{\lambda_1}{\lambda_2-\lambda_1}}(\psi_1 - \psi_2) \tag{20}$$

$$\text{because } e^{-i\pi\frac{\lambda_2}{\lambda_2-\lambda_1}} = e^{-i\pi\frac{\lambda_2-\lambda_1}{\lambda_2-\lambda_1}}e^{-i\pi\frac{\lambda_1}{\lambda_2-\lambda_1}} = -e^{-i\pi\frac{\lambda_1}{\lambda_2-\lambda_1}} \tag{21}$$

which means that at $t' = \tau$ we have the negative combination of ψ_1 and ψ_2 that is completely concentrated on the left side (see Fig. 2 right). There is also an additional phase but it is not changing the squared module.

2.1 Root-finding

The eigenvectors with eigenvalues $0 < \lambda < v_0$ of the Hamiltonian are the solution of the following equation

$$f(\lambda) = e^{\kappa/3}\left[\kappa\sin\left(\frac{k}{3}\right) + k\cos\left(\frac{k}{3}\right)\right]^2 - e^{-\kappa/3}\left[\kappa\sin\left(\frac{k}{3}\right) - k\cos\left(\frac{k}{3}\right)\right]^2 = 0 \tag{22}$$

where $k = \sqrt{\lambda}$ and $\kappa = \sqrt{v_0 - \lambda}$

The function is represented in Fig. 3, where we can see that there are oscillations and the value of the function decreases and cross the axis $y = 0$ and then increase value immediately

after, giving solutions in close pairs at values near to the numerical solutions. In fact, a root-finding algorithm was implemented to find solutions of the equation, starting from one of the numerical eigenvalues in each pair and finding the closest minimum. This will correspond to a negative value of the function and it is used as starting point to find the roots using bisection method on each side of the minimum. The results are presented in Tab. 1.

	$n=1$	$n=2$	$n=3$	$n=4$	$n=5$	$n=6$
Numerical roots λ_n	73.936	73.938	293.492	293.516	648.264	648.750
λ_n $(N=100)$	73.076	73.078	289.722	289.748	638.960	639.435
λ_n $(N=1000)$	73.866	73.868	293.217	293.241	647.667	648.154
λ_n $(N=10000)$	73.929	73.931	293.466	293.490	648.208	648.694

Table 1: Numerical roots and numerical eigenvalues compared for different values of N.

From Fig. 3 it is clear that increasing V_0 increases the oscillations and the number of solutions with $0 < \lambda < v_0$ whereas decreasing it has the opposite effect. There will be a point where all the eigenvalues will be at energy $\lambda \geq v_0$. To find this limit, let us define $A = \kappa \sin\left(\frac{k}{3}\right)$ and $B = k\cos\left(\frac{k}{3}\right)$ and rewrite Eq. 22

$$e^{\kappa/3}\left[A+B\right]^2 - e^{-\kappa/3}\left[A-B\right]^2 = 0 \tag{23}$$

$$2(A^2+B^2)\sinh\left(\frac{\kappa}{3}\right) + 4AB\cosh\left(\frac{\kappa}{3}\right) = 0 \tag{24}$$

$$4\kappa k \sin\left(\frac{k}{3}\right)\cos\left(\frac{k}{3}\right) = 0 \tag{25}$$

$$\cos\left(\frac{k}{3}\right) = 0 \implies \frac{k}{3} = \frac{\pi}{2} \implies \lambda = \frac{9\pi^2}{4} \approx 22.2 \tag{26}$$

In the derivation, we are considering the case of solutions in the limit of $\lambda \to v_0$ and in that case both κ and $\sinh\left(\frac{\kappa}{3}\right)$ will go to zero. We are left with the term in $\cosh\left(\frac{\kappa}{3}\right)$, that will instead go to 1 so we need to have $4AB = 0$ and by substituting we find that the non zero solution is at $\lambda = \frac{9\pi^2}{4} \approx 22.2$. From Fig. 3 we can see that in fact for $v_0 = 23, 24$ we still have a solution very close but lower than v_0 but for $v_0 = 22$ the only solutions are at exactly $\lambda = 0, v_0$, that are out of the range of validity of the equation.

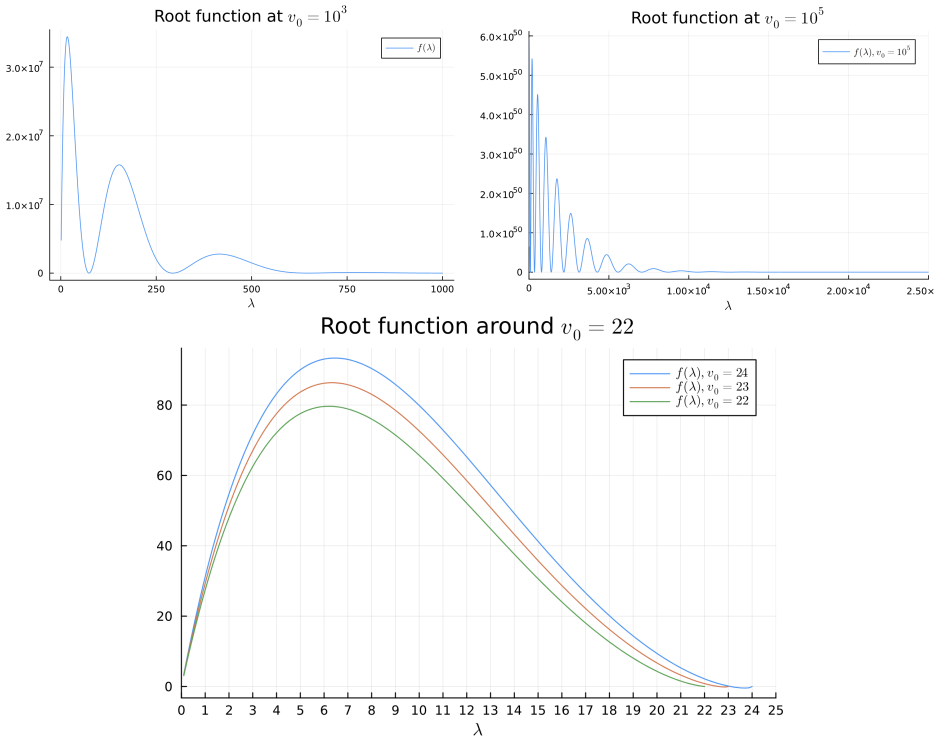

Figure 3: Plots of function in Eq. 22 for different values of v_0.

2.2 Step-by-step time evolution

To describe the evolution of the wave function in time, let's try a different approach. After a small time $\Delta t'$ the solution of Eq. 11 can be expressed as

$$\Psi(x', t' + \Delta t') = \exp\left(-i\Delta t' \hat{H}'\right) \Psi(x', t') \approx \left(1 - i\Delta t' \hat{H}'\right) \Psi(x', t') \tag{27}$$

where we used the Taylor expansion to the first order of the exponential, assuming that $\Delta t'$ and thus the exponent is very small. The forward Euler method arising from this derivation is implemented but after several time steps or too-large time-steps, it is clear that the L2 norm of the wavefunction is not conserved. Looking at the animation [3], we see that even if for some steps the variation of the norm is quite small, at some point the function completely disrupts and give very high values of L2 norm. Keeping $\Delta x' = 0.01$, choosing $\Delta t' = 10^{-5}, 10^{-4}, 10^{-3}$ gives variations on the L2 norm of the solution of $2.6 \cdot 10^{-7}, 2.6 \cdot 10^{-5}, 2.6 \cdot 10^{-3}$ respectively, which means the errors are $O(\Delta t'^2)$.
This is due to the fact that the approximated evolution is not unitary. A better approximation will be to use

$$\exp\left(-i\Delta t' \hat{H}'\right) = \frac{1 - \frac{i}{2}\Delta t' \hat{H}'}{1 + \frac{i}{2}\Delta t' \hat{H}'} \tag{28}$$

This allow to keep the unitary property of the operator and gives a Crank-Nicolson scheme, that is also implemented in the code

$$\left[1 + \tfrac{i}{2}\Delta t' \hat{H}'\right] \Psi(x', t' + \Delta t') = \left[1 - \tfrac{i}{2}\Delta t' \hat{H}'\right] \Psi(x', t') \tag{29}$$

In this case, from the animation [4] is clear that the squared module is conserved.
When the initial condition can be expressed in an easy and finite form with the expansion in

eigenfunctions, then the scheme of Sec. 1.4 only require to only evaluate a linear combination of the eigenfunctions with the coefficients α_n, determined only once, and the exponential with the eigenvalues. The method presented in this section instead require a matrix-vector multiplication, with a matrix that needs to be evaluated the first time, but never evaluates the eigenfunctions and eigenvalues. Also, for the case of an initial condition of a delta centered in $x = 0.5$, we don't have the limitation of its description as expansion of a finite basis that was problematic in the first method.

3 Periodic detuning of a two-level system

We will now consider the case of a lower barrier, followed by another barrier or well of variable amount.

$$V(x) = \begin{cases} 0, & \text{for} \quad 0 \leq x < L/3 \\ V_0, & \text{for} \quad L/3 \leq x < 2L/3 \\ V_1, & \text{for} \quad 2L/3 \leq x < L \\ \infty, & \text{otherwise} \end{cases} \tag{30}$$

We set $v_0 = 100$ and scan the two lowest eigenvalues varying v_1 from -500 to $+500$. The results are presented in Fig. 4.

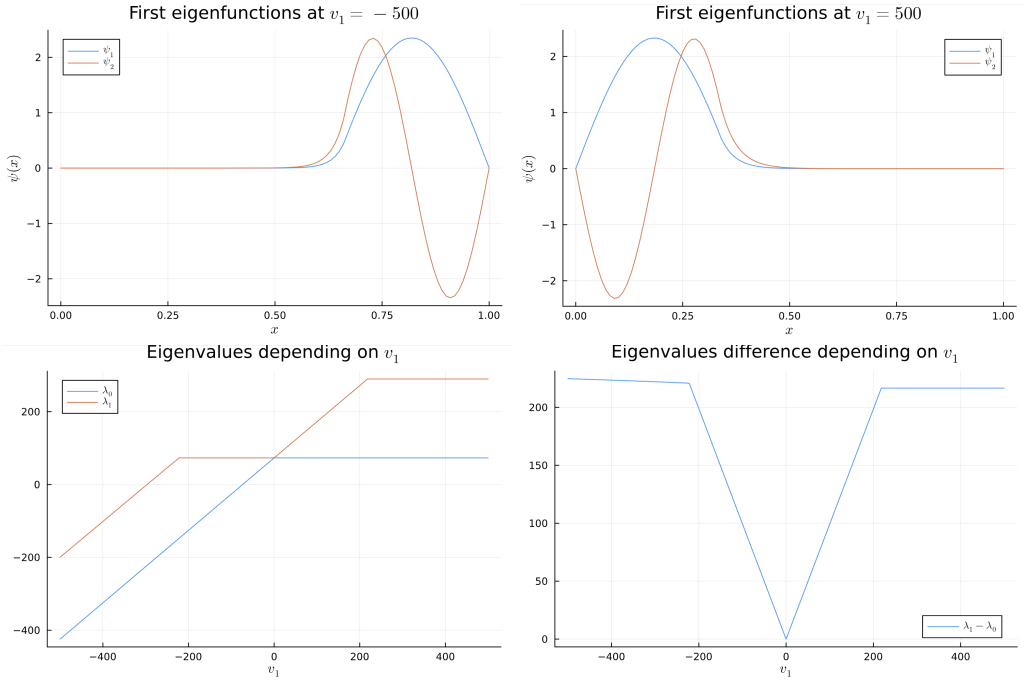

Figure 4: (Top) First 2 eigenfunctions choosing $v_1 = -500$ (left) and $v_1 = 500$ (right) (Bottom) First two eigenvalues at different values of v_1 from -500 to 500 (left) and their difference (right).

The energy of the ground state λ_1 is constant for positive values of V_1 and then steadily decrease for negative values. For high V_1 values, the ground state is localized to the left of the barrier, where the potential is constantly zero and thus the energy doesn't change. For high negative values it is instead localized in the well and the potential continually decrease, making λ_1 decrease as well. The energy difference between the ground state and excited state are also shown in Fig. 4 (bottom right), where we can see that there is a minimum

when $V_1 = 0$ with energy difference $\lambda_0 = 0.002197$ (from Sec. 1.1, $\varepsilon_0 = \hbar\lambda_0/t_0$).
This behaviour can be modeled by a simple 2x2 effective Hamiltonian, shifted by $-\lambda_0/2$

$$\hat{H}_{\text{eff}} = \begin{pmatrix} -\lambda_0/2 & \tau \\ \tau & \lambda_0/2 \end{pmatrix} \tag{31}$$

The tunneling amplitude τ can be obtained by evaluating the matrix element of the Hamiltonian, that is

$$\tau = \langle g_0 | \hat{H}_{\text{eff}} | e_0 \rangle = \int_0^1 \mathrm{d}x' \, \psi_0(x') \left(-\frac{\partial^2}{\partial x'^2} + v(x', v_1) \right) \psi_1(x') \tag{32}$$

where $|g_0\rangle$ and $|e_0\rangle$ are the ground state and excited state at $v_1 = 0$. From the definition is clear that τ is a function of v_1. In particular when $v_1 = 0$, then ψ_1 will be an eigenfunction of the Hamiltonian in parenthesis and thus return itself times the eigenvalue and eventually give zero when projected on the orthogonal eigenfunction ψ_0. The integral is evaluated using the trapezoidal rule and the results for $\tau(v_1)$ are presented in Fig. 5.

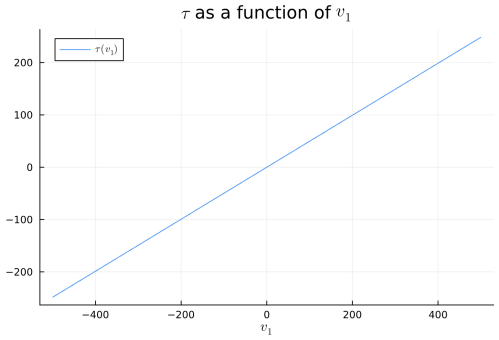

Figure 5: Plot of tunneling amplitude τ at different values of v_1, using Eq. 32.

It looks like the plot follow the equation $\tau(v_1) = v_1/2$. In fact, we can break the integral in Eq. 32 in a term that contains the kinetic term and only the barrier v_0 and another term with the potential v_1 in $2/3 \leq x < 1$ and zero everywhere else. The first terms is the actual Hamiltonian for ψ_0 and ψ_1 and gives zero and the second one instead gives a contribution. By looking at the eigenfunctions in Fig. 2 (right), we can see that in the interval where the integral is evaluated, the two eigenfunctions are equal, which means we are integrating the squared module of the eigenfunction on an interval that includes only half of the contribution, giving a final value of a half.

$$\tau = \int_0^1 \mathrm{d}x' \, \psi_0(x') \left(-\frac{\partial^2}{\partial x'^2} + v(x', v_1) \right) \psi_1(x') = 0 + v_1 \int_{2/3}^1 \mathrm{d}x' \, \psi_0(x') \psi_1(x') \approx v_1 \frac{1}{2} \tag{33}$$

This is not exact since the integral of the squared module is not exactly zero in $[1/3, 2/3]$ so the final value is not exactly the half of the total integral of the module squared, but a little less than that. By actually looking at the numerical values, we find $\tau(v_1) = 0.4968\, v_1$

3.1 Rabi oscillations

(NOTE: In order to get rid of $\hbar$, this section will be all treated using the notation of Sec. 1.1 even without an explicit prime symbol, unless specified differently. The equations have been adapted with respect to the ones in the assignment)
We can now move to a time-dependent Hamiltonian, where we are modulating the value of

the potential and thus the tunneling amplitude in resonance with the energy splitting λ_0 but with values of τ very small compared to λ_0. The Hamiltonian is then expressed as

$$\hat{H}_{\text{eff}} = \begin{pmatrix} -\lambda_0/2 & \tau\sin(\omega t) \\ \tau\sin(\omega t) & \lambda_0/2 \end{pmatrix} \tag{34}$$

In order to solve this Hamiltonian we need to keep track of the time-dependence that is in the Hamiltonian and in the state vectors. In this case we get the Schrödinger equation in the interaction picture that reads

$$i\frac{d}{dt}\left|\psi(t)\right\rangle_I = \hat{H}_{1I}(t)\left|\psi(t)\right\rangle_I \tag{35}$$

where now the interaction Hamiltonian is

$$\hat{H}_{1I}(t) = \begin{pmatrix} 0 & e^{-i\lambda_0 t}\tau\sin(\omega t) \\ e^{i\lambda_0 t}\tau\sin(\omega t) & 0 \end{pmatrix} \tag{36}$$

which gives a formal solution of Eq. 35 as

$$\left|\psi(t)\right\rangle_I = \left|\psi(0)\right\rangle - i\int_0^t \mathrm{d}t'\,\hat{H}_{1I}(t')\left|\psi(t')\right\rangle_I \tag{37}$$

To obtain a discrete form of the integral, let us consider the state $\left|\psi(t)\right\rangle_I$ as an array of n pairs $\left|\psi(t=k\Delta t)\right\rangle_I$, $k = 0, 1, \ldots, n$ that are the projection onto the ground state and excited state. Using trapezoidal rule for the integral, the expression for $t = \Delta t$ reads

$$\begin{pmatrix}\psi_1(\Delta t)\\ \psi_2(\Delta t)\end{pmatrix} = \begin{pmatrix}\psi_1(0)\\ \psi_2(0)\end{pmatrix} - i\frac{\Delta t}{2}\left[\hat{H}_{1I}(0)\begin{pmatrix}\psi_1(0)\\ \psi_2(0)\end{pmatrix} + \hat{H}_{1I}(\Delta t)\begin{pmatrix}\psi_1(\Delta t)\\ \psi_2(\Delta t)\end{pmatrix}\right] \tag{38}$$

where $\left|\psi_1(0)\right\rangle = \left|g_0\right\rangle\left\langle g_0|\psi(0)\right\rangle$ and $\left|\psi_2(0)\right\rangle = \left|e_0\right\rangle\left\langle e_0|\psi(0)\right\rangle$. We can move all the terms with $(\psi_1(\Delta t),\, \psi_2(\Delta t))$ on the LHS and generalize the equation using trapezoidal rule to discretize the integral into $\Delta t(f_0/2 + f_1 + ... + f_{k-1} + f_k/2)$

$$\hat{M}_k \cdot f_k = f_0 + \sum_{l=0}^{k-1}\hat{N}_l \cdot f_l \tag{39}$$

where

$$\hat{N}_k = \begin{pmatrix} 0 & -i\Delta t e^{-i\lambda_0 k\Delta t}\tau\sin(\omega k\Delta t) \\ -i\Delta t e^{i\lambda_0 k\Delta t}\tau\sin(\omega k\Delta t) & 0 \end{pmatrix}, \tag{40}$$

$$\hat{M}_k = I_{2\text{x}2} - \frac{1}{2}\hat{N}_k, \quad f_k = \begin{pmatrix}\psi_1(k\Delta t)\\ \psi_2(k\Delta t)\end{pmatrix} \tag{41}$$

The method is implemented in the code, starting with $f_0 = (1, 0)$ in order to start with the system in the ground state. The other important parameters are $\lambda_0 = 0.002197$ (from the previous case), $\tau = 0.02\lambda_0$ and $\omega = \lambda_0$ to have the modulation of the tunneling amplitude in resonance. We observe that increasing time makes the coefficient of the ground state decrease and the coefficient of the excited state increase, and eventually swap with each other periodically. It is interesting to look at the probability to find the system in the state $\left|e_0\right\rangle$ at a time $t > 0$. This probability is defined as

$$p(t) = \left|\langle e_0|\psi(t)\rangle\right|^2 \implies p(k\Delta t) = \left|f_{k,2}\right|^2 \tag{42}$$

The two characteristic times in the method are the period of $\sin^2(\omega t)$ that is $T_1 = \pi/\omega \approx 1430$, and the period for the tunneling cycle related to τ that is $T_2 = 2\pi/\tau \approx 1.43\,10^5$. This

last one can be better understood by averaging the contributions that rotate very fast, with period T_1, and only keep the ones with period T_2. Within this approximation there is an analytical solution for the probability, which has period T_2

$$p(t) = \sin^2\left(\frac{t\tau}{2}\right) \tag{43}$$

The probability is shown in Fig. 6, for both the numerical solution and the averaged analytical solution. On the left plot we have times of the order of T_1 and the probability increases with some oscillations due to $\sin(\omega t)$ that are instead averaged in the analytical solution. On the right instead the times are of the order of T_2 and it is possible to appreciate the cycles of the shift in probability between ground state and excited state, that swaps every $T_2/2$. The fast oscillations are still slightly visible for the numerical solution.

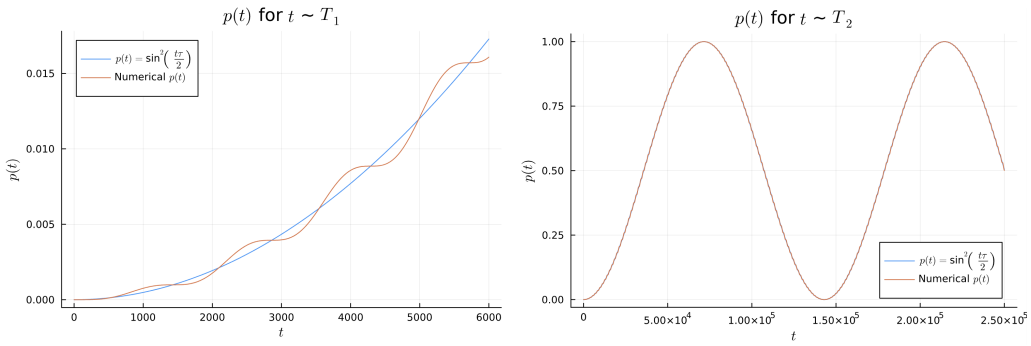

Figure 6: Plots of the probability to find the system in the state $|e_0\rangle$. (Left) The solutions are obtained choosing $\Delta t = 5$ for 1200 steps. (Right) The solutions are obtained choosing $\Delta t = 5$ for 50000 steps.

Changing the frequency even a little makes large differences in the results, as can be seen in Fig. 7. In particular decreasing the frequency to $0.95\lambda_0$ (or increasing it to $1.05\lambda_0$) keeps the fast oscillations almost unchanged, with a period that is only changed by the same 5%. The slower ones are now significantly faster and $p = 1$ is never reached, the probability oscillates between 0 and 0.13. The analytical averaged solutions is not appropriate to describe this situation. Increasing τ at resonance instead makes the period of the two oscillations similar and the results contains oscillation that are much more complex since the phases interacts with each others and the assumption of slow and fast oscillation is not true anymore.

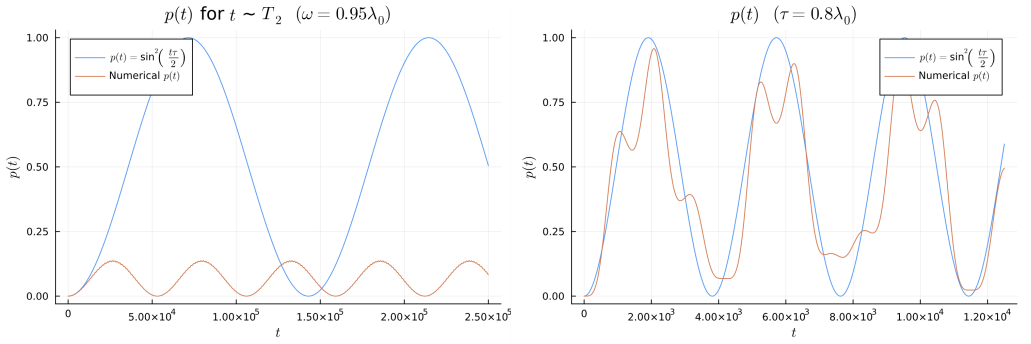

Figure 7: Plots of the probability to find the system in the state $|e_0\rangle$. (Left) The solutions are obtained choosing $\Delta t = 50$ for 5000 steps. (Right) The solutions are obtained choosing $\Delta t = 5$ for 2500 steps.

Animations on GitHub

(1) https://github.com/FedeRoxx/ComputationalPhysics/blob/main/Assignment_2/Time_evolution_delta.gif.

(2) https://github.com/FedeRoxx/ComputationalPhysics/blob/main/Assignment_2/Time_evolution_barrier.gif.

(3) https://github.com/FedeRoxx/ComputationalPhysics/blob/main/Assignment_2/Time_evolution_barrier_FE.gif.

(4) https://github.com/FedeRoxx/ComputationalPhysics/blob/main/Assignment_2/Time_evolution_barrier_CN.gif.